

A SERVO-CONTROLLED CAPACITIVE PRESSURE SENSOR WITH A THREE-MASK FABRICATION SEQUENCE

Jae-Sung Park*, and Yogesh B. Gianchandani¹

Department of Electrical and Computer Engineering

*Department of Mechanical Engineering
University of Wisconsin, Madison, USA

ABSTRACT

A Si micromachined servo-controlled capacitive pressure sensor is described. The use of a capped-cylinder shape with pick-off electrodes external to a sealed cavity permits this device to be fabricated in only three masking steps. Device behavior is evaluated experimentally and by finite element analysis. A fabricated device with 2 mm diameter, 9.7 μm structural thickness and 10 μm cavity height provides a measured sensitivity of 0.516 V/kPa over a dynamic range of 20-100 kPa gauge pressure, with a non-linearity of <3.22% of full scale. The open-loop sensitivity of this device averaged over a dynamic range of 0-250 kPa is -408 ppm/kPa. A voltage bias applied to the servo-electrode can be used to tune both the open-loop and closed-loop sensitivity by more than 30%.

Keywords: Pressure sensor, servo-control, electrostatic actuation

1. INTRODUCTION

Micromachined capacitive pressure sensors generally operate by sensing the downward displacement of a thin, flexible diaphragm using an electrode located beneath it [1]. They tend to provide higher sensitivity, lower temperature coefficients, and lower power consumption than piezoresistive pressure sensors, which sense the deformation of a diaphragm by changes in stress at various locations on its surface. For these benefits, capacitive pressure sensors tend to compromise linearity and/or dynamic range.

Closed-loop operation of a sensor can potentially improve dynamic range and linearity, and also suppress noise. A few servo-controlled pressure sensors have been reported in recent years [2,3]. Typically, the pressure-induced deflection of the diaphragm is balanced by an opposing electrostatic force, which is a natural choice when a capacitive pick-off already exists in the device, but faces two constraints. The first is that applied voltages provide only attractive forces. This adds design and fabrication complexity because another actuation electrode must be located above the diaphragm. Past efforts have used double-sided wafer processing or as many as 15 masking steps (including device

encapsulation). The second constraint is that for voltages smaller than the pull-in voltage (at which the diaphragm collapses to the actuating electrode), the electrostatic pressure is smaller than the external pressure. To compensate for this, the servo-actuation electrode must be larger than the flexible diaphragm [3].

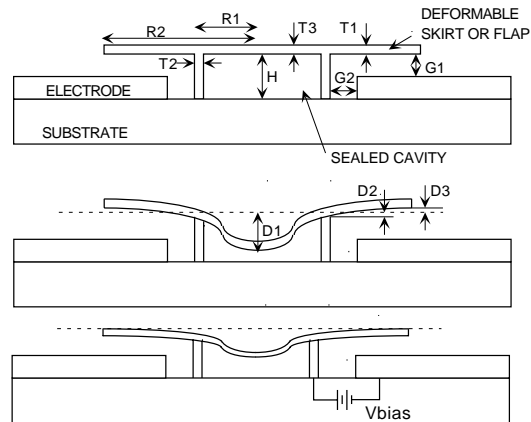


Fig. 1: Electrostatic attraction between the electrode and skirt opposes the deflection due to external pressure.

Although the area constraint cannot be easily circumvented, the fabrication complexity of a closed loop pressure sensor can be simplified using an unconventional device structure. This paper reports on the servo-controlled operation of a pressure sensor fabricated by a 3-mask process. The structure is similar to an open loop pressure sensor reported in [4,5]. As illustrated in Fig. 1, this device includes a sealed cavity formed between the substrate and a diaphragm that extends outward to form a deformable skirt or flap. In open-loop operation, as the external pressure increases, the center of the diaphragm is deflected *downward* while the skirt is deflected *upward*. This movement is sensed capacitively by an electrode located underneath the skirt. The location of the sense electrode eliminates the need for lead transfer from inside the sealed cavity. More importantly for closed loop operation, it permits the deflection of the skirt to be balanced by a voltage bias on the sense electrode. A separate actuation electrode located above the diaphragm is unnecessary. Moreover, the concentric layout of the sealed cavity and the skirt

¹ Address: 1415 Engineering Drive, Madison, WI 53706-1691, USA; Tel: (608) 262 2233; Fax: (608) 262 1267; E-mail: yogesh@engr.wisc.edu

permits the electrode to naturally occupy a larger area than the diaphragm, as preferred for electrostatic feedback. A point of distinction from other implementations is that in this feedback scheme the skirt, and not necessarily the diaphragm, is restored to its reference position. The resulting performance is evaluated in the following sections.

II. MODELING

The finite element analysis (FEA) of the open-loop response for this pressure sensor was presented in [4,5]. Setting dimensional variables as defined in Fig. 1, T1(skirt thickness)= T2(sidewall thickness)= T3 (diaphragm thickness)= 5 μm , R1(cavity radius)= 500 μm , R2(skirt radius)= 1000 μm , H(cavity height)= 30 μm , and G1(capacitor gap)= 5 μm , simulations using ANSYSTM software indicated that neutral capacitance was approximately 3.8 pF, while the open-loop sensitivity was -2900 ppm/kPa when the diaphragm was not in contact with the substrate, i.e., in non-touch mode, and -270 ppm/kPa in touch mode. The temperature coefficient of offset (TCO) was 80 ppm/K in non-touch mode, while the temperature coefficients of sensitivity (TCS) were 77 and 31 ppm/K in the non-touch and touch modes, respectively. The assumptions used in the expansion mismatch between the structural and substrate materials limit the applicability of these estimates to the vicinity of room temperature.

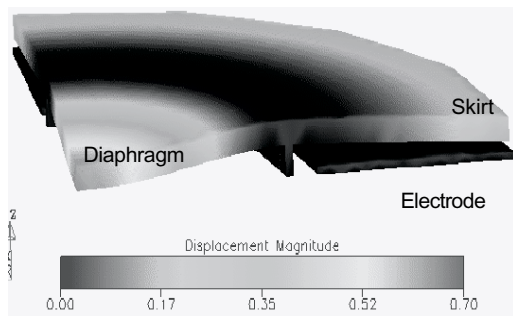


Fig. 2: Simulated shape of the sensor in closed loop operation. The deformation is exaggerated by 10x.

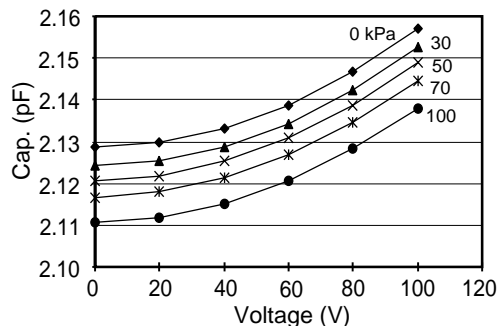


Fig. 3: Simulated feedback actuation over various pressures applied across the diaphragm.

Coupled-field analysis is necessary to model the closed-loop response of the pressure sensor, since both pressure and electrostatic forces must be simulated. Using MEMCADTM software, a structure with dimensions T1= T2= T3= 10 μm , R1= 500 μm , R2= 1 mm, H=10 μm , and G1= 9 μm , was meshed with a 10-node tetrahedral element. The dimensions of this device are better suited to closed-loop operation. The deformed shape is shown in Fig. 2, whereas the change in device capacitance with applied bias, which characterizes the feedback actuation, is plotted in Fig. 3 for various pressures across the diaphragm. The calculated pull-in voltage was $>100\text{V}$, the neutral capacitance was 2.13 pF, and the closed-loop sensitivity was 0.64 V/kPa from 20 kPa to 90 kPa. The overall response is compared to measurements in section IV.

III. FABRICATION

The device was fabricated by the three-mask dissolved wafer process, as described in [5,6]. A Si wafer is first dry-etched to define the sidewall of the sealed cavity, then selectively diffused with boron to define the radius of the pressure sensor. The Si wafer is then flipped over and anodically bonded to a glass wafer that has been inlaid with a Ti/Pt metal pattern that serves as interconnect and provides the bond pads. The undoped Si is dissolved in a dopant-selective etchant. The lead transfer is facilitated by a protrusion in the sidewall and a notch in the diaphragm that surrounds it [5]. A reference device can be made with a breach in the sidewall. Figure 4 shows images of fabricated devices.

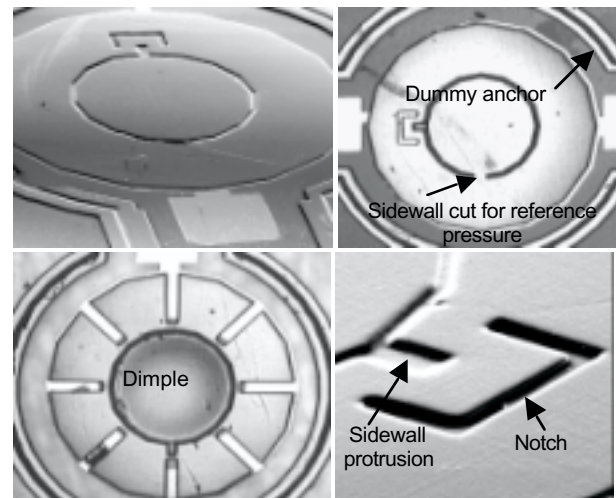


Fig. 4: (a-upper left) SEM image of a fabricated device; (b-upper right) optical image of reference sensor with sidewall breach; (c-lower left) dimpled diaphragm showing a sealed cavity; (d-lower right) protrusion and notch for lead transfer.

A point of interest in fabricating the device pertains to the shear force due to expansion mismatch between the glass and Si wafers [7]. The force generated is:

$$F_{sg} = \frac{(\alpha_s - \alpha_g) \bullet \Delta T}{\left(\frac{1}{E_s t_s} - \frac{1}{E_g t_g} \right)} \quad (1)$$

where ΔT is the difference between the bonding temperature and operating temperatures, α , E , and t denote the expansion coefficient, Young's modulus, and thickness of the wafers. The subscripts s and g denote Si and glass, respectively. Since the bonded area in the device is only the footprint of the cavity sidewall, the shear force is sustained by a small area. This can lead to failure manifested as cracks in the glass as the wafers are cooled after anodic bonding. However, it is evident from eqn. (1) that reducing the wafer thickness can alleviate this problem. It is convenient to chemically thin the Si wafer prior to bonding. Figure 5 shows the shear stress (F_{sg} per unit bond area) as a function of the thickness of the Si wafer. These calculations assume that $\alpha_s = 2.3$ ppm/K, $\alpha_g = 1.3$ ppm/K, $\Delta T = 300^\circ\text{C}$, $E_s = 160$ GPa, $E_g = 73$ GPa, $t_g = 600$ μm , and the width of bonding surface is 15 μm . Dummy anchors around the device also reduce stress. When the Si wafer was chemically thinned prior to bonding, the device yield was >80% with Corning #7740 glass as a substrate.

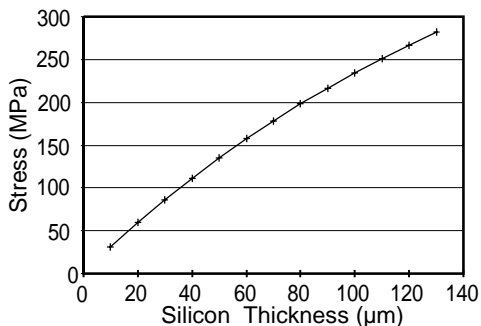


Fig. 5: Calculated shear stress at the bonding surface.

IV. MEASUREMENTS

Tests were performed on unpackaged devices placed within a test chamber. All measurements (Figs. 6-9) are referenced to the gauge pressure within the chamber, which was measured by a Motorola MPX5100DP pressure sensor device (upto 100 kPa). The capacitance was measured by a Kiethley 590 CV Analyzer.

Due to equipment constraints, the cavity was sealed at atmospheric pressure at the bonding temperature of 500-550 $^\circ\text{C}$. This corresponds to ≈ 37 kPa pressure at room temperature. However, the pressure within the sealed cavity may be higher because of out gassing from

the glass substrate. Entrapped gas can significantly increase the apparent temperature coefficients of the pressure sensor. However, commercially available bonding equipment and the use of a thin-film getters provide proven solutions to these problems [8].

The open-loop measurement of a fabricated device with $T1 = T3 = 9.7$ μm , $T2 = 18$ μm , $H = 10$ μm , $R1 = 500$ μm , and $R2 = 1$ mm is shown in Fig. 6. The average sensitivity obtained by a least squares fit over the entire tested range of 250 kPa is -408 ppm/kPa, with a reading of 2.91 pF at zero gauge pressure. Despite the wide dynamic range used in the test, no hysteresis was observed in the response, demonstrating that fracture strength was not exceeded. A smaller device on the same wafer with $R1 = 300$ μm and $R2 = 600$ μm showed a sensitivity of -101 ppm/kPa with 0.988 pF at zero gauge pressure.

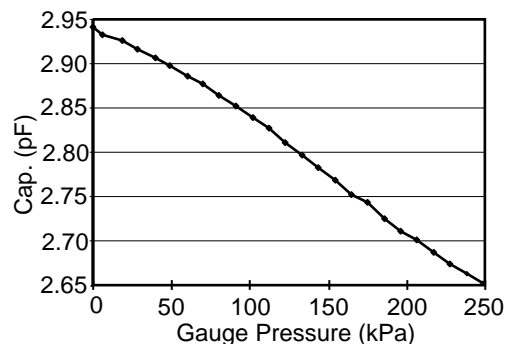


Fig. 6: Measured response in open-loop operation.

In preparation for closed loop measurements, the response of the 2 mm diameter device was characterized by measuring the capacitance change with applied pressure under varying bias voltages (Fig. 7) and the capacitance change with applied bias at various pressures (Fig. 8). These figures respectively show the range of parameterized interaction between the applied pressure and the applied voltage bias. Closed loop operation of the pressure sensor was demonstrated by varying the chamber pressure and setting the bias voltage to provide the capacitance that was measured at zero gauge pressure. As shown in Fig. 9, the applied voltage was varied from 31.2-73.2 V as the pressure was varied from 20-100 kPa, providing an average sensitivity 0.516 V/kPa. Over this range the response deviates from linearity by $\leq 3.22\%$ of the full scale output.

In addition to the measured results, Fig. 9 shows the output predicted by FEA. For gauge pressure lower than 60 kPa, the match is clearly very good. At larger pressures there is a deviation, possibly because the tetrahedral element that was used in FEA is structurally stiffer than the real value, and large deviation analysis was not accurate.

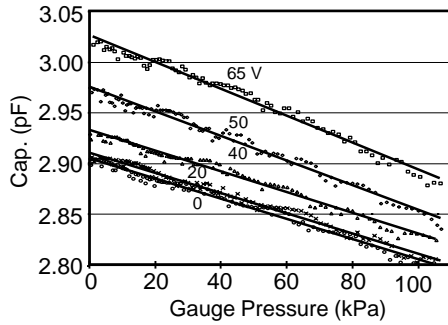


Fig. 7: Device response with various bias voltages.

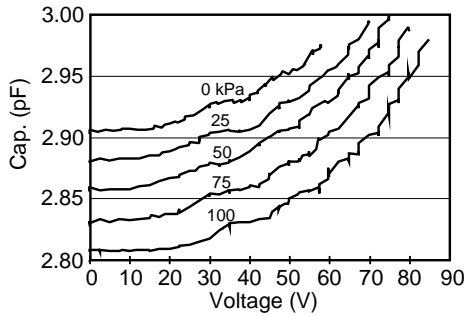


Fig. 8: Electrostatic deflection at various pressures.

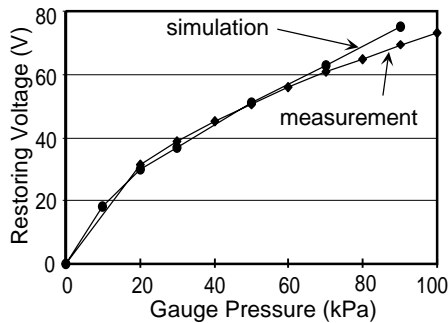


Fig. 9: Closed-loop response of the pressure sensor.

V. DISCUSSION

The results presented in section IV demonstrate the closed-loop operation of the pressure sensor. There are several points worth noting about the design and operation of this device.

First, for the dimensions that were selected, the closed-loop sensitivity was 0.516 V/kPa, which necessitated a 73.2 V bias for a dynamic range of 100 kPa. The bias can be reduced by increasing the diameter of the skirt or by reducing the capacitive gap between it and the electrode. As explained in [5], the gap may be reduced by increasing the thickness of the deposited metal that forms the electrode (e.g., by electroplating); reducing the cavity height is not recommended because it reduces the overall compliance of the Si structure, and depending on the dimensions used, may result in lower sensitivity. Reducing the capacitive gap would increase the non-linearity of the open-loop response.

Second, the sensitivity of the closed-loop response can be electronically tuned. It can be seen from Fig. 8 that a 100 kPa dynamic range requires a bias swing of 0-73 V if the reference capacitance is 2.91 pF. However, at 2.96 pF, the 0-100 kPa range requires a swing of only 53.9-82.3 V, which corresponds to a sensitivity of 0.284 V/kPa. This may be implemented, for example, by biasing the Si structure at -68 V and modulating the electrode voltage over a range of ± 15 V. The advantage of this implementation is that standard electronics may be used for the servo-operation, while the bias supply, which is out of the loop, serves as a control parameter that could compensate for variations in manufacturing or operating conditions.

Third, the bias between the structure and electrode may also be used to tune the open-loop response. Figure 7 shows the average open-loop sensitivity over a 0-105 kPa dynamic range changes from -328 ppm/kPa to -437 ppm/kPa (a 33% increase) while the reference capacitance changes from 2.91 pF to 3.03 pF as the bias increases from 0-65 V. (Note that the zero-bias sensitivity of -408 ppm/kPa obtained from Fig. 6 was averaged over a much wider dynamic range of 250 kPa.)

Continuing efforts on this project focus on packaging the devices in an inert liquid with a relatively high dielectric constant, which will further increase the output capacitance, making the readout even easier.

REFERENCES

- [1] A.V. Chavan, K.D. Wise, "A monolithic fully integrated vacuum sealed CMOS pressure sensor," *Proc., IEEE MEMS 2000*, Miyazaki, pp. 341-6
- [2] Y. Wang, M. Esashi, "A novel electrostatic servo capacitive vacuum sensor," *Proc., IEEE Transducers 1997*, Chicago, pp. 1457-60
- [3] B.P. Gogoi, C.H. Mastrangelo, "A low-voltage force-balanced pressure sensor with hermetically sealed servomechanism," *IEEE MEMS 1999*, Orlando, pp. 493-8
- [4] J.-S. Park and Y.B. Gianchandani, "A low-cost batch sealed capacitive pressure sensor," *Proc., IEEE MEMS 1999*, Orlando, pp. 82-87
- [5] J.-S. Park, Y.B. Gianchandani, "A capacitive absolute-pressure sensor with external pick-off electrodes," *J. Micromech. & Microeng.*, 10(4), Dec. 2000, pp. 528-533
- [6] Y.B. Gianchandani, K. Najafi, "A bulk silicon dissolved wafer process for microelectromechanical devices," *IEEE J. Microelectromechanical Sys.*, 1(2), June 1992, pp. 77-85
- [7] W.H. Ko, J.T. Suminto, G.J. Yeh, "Bonding techniques for microsensors," *Micromachining and Micropackaging of Sensors*, 1985, Elsevier Science, and *Microsensors*, Ed. R.S. Muller, et al, 1990, IEEE Press, pp. 198-208
- [8] Y.T. Cheng, W.T. Hsu, L. Lin, C.T. Nguyen, K. Najafi, "Vacuum packaging technology using localized aluminum/silicon-to-glass bonding," *Proc., IEEE MEMS 2001*, Interlaken, pp. 18-21